

# Quantifying Device Flexibility With Shapley Values in Demand Side Management

Ivo A. M. Varenhorst  
University of Twente  
Enschede, the Netherlands  
i.a.m.varenhorst@utwente.nl

Marco E. T. Gerards  
University of Twente  
Enschede, the Netherlands  
m.e.t.gerards@utwente.nl

Johann L. Hurink  
University of Twente  
Enschede, the Netherlands  
j.l.hurink@utwente.nl

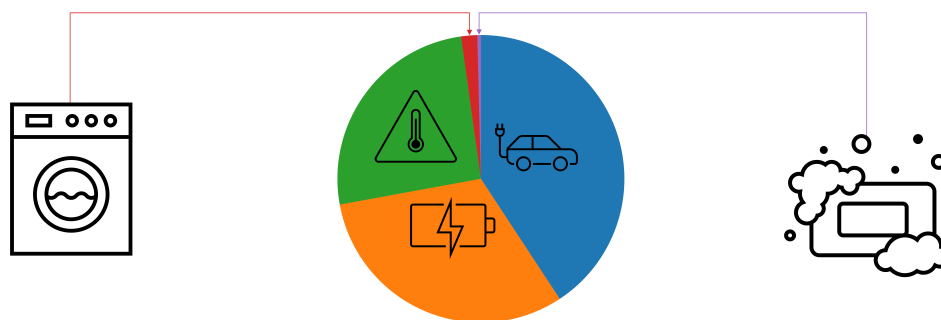


Figure 1: Shapley value pie chart of an electric vehicle, a home battery, a heat pump, a washing machine and a dishwasher.

## ABSTRACT

The value of flexibility in demand side management (DSM) is a measure that is hard to quantify. However, having such a value is important in various areas, from determining research directions to cost allocation and writing policy. In this work, we propose a method to determine the value of flexible assets using average marginal contributions, based on the Shapley value. We apply this method in a smart home peak shaving DSM context. Our results show that the Shapley value of an electric vehicle (EV) is the largest in this context, 27% larger than the Shapley value of the runner-up, a battery energy storage system. This highlights that when doing research or writing policy for DSM in the residential sector, EVs are the most important area to focus on. Additionally, we show that if the right device configurations are chosen, there can be strong synergy between devices, i.e., the flexibility valuation of combinations of devices can be higher than the sum of their individual contributions. The results of this work provide intuition for which device configurations and combinations can achieve such synergy. The presented framework can not only be used to value flexible assets in DSM in the context of a smart home, but can also be applied to larger scale energy systems.

## CCS CONCEPTS

• Hardware → Smart grid; Energy metering.



This work is licensed under a Creative Commons Attribution International 4.0 License.

E-Energy '24, June 04–07, 2024, Singapore, Singapore  
© 2024 Copyright held by the owner/author(s).  
ACM ISBN 979-8-4007-0480-2/24/06  
<https://doi.org/10.1145/3632775.3661950>

## KEYWORDS

Demand side management (DSM), Energy management, Energy flexibility, Optimization, Shapley values

## ACM Reference Format:

Ivo A. M. Varenhorst, Marco E. T. Gerards, and Johann L. Hurink. 2024. Quantifying Device Flexibility With Shapley Values in Demand Side Management. In *The 15th ACM International Conference on Future and Sustainable Energy Systems (E-Energy '24)*, June 04–07, 2024, Singapore, Singapore. ACM, New York, NY, USA, 11 pages. <https://doi.org/10.1145/3632775.3661950>

## 1 INTRODUCTION

The European Commission's carbon emission targets for 2050 require large-scale integration of renewable energy sources (RES). For the integration of these devices in the energy system, energy management is required. Flexible assets should be controlled to temporally shift their load to time frames where renewable energy is available [4]. Demand side management (DSM) and demand response (DR) are technologies enabling this use of flexibility. As an illustration of their potential, a Norwegian study found that in the future 2050 grid, "DR may contribute to peak shaving of up to 18.6% of total peak load" in the Northern European energy system [21], which they estimate is a peak reduction of 16.9 GW by DR alone. Söder et al. [29] also reviewed the potential of demand side flexibility in Northern Europe, and found that in 2018 already, the potential flexibility amounted to 15-29% of the peak power in the system. Thus, DR and DSM are interesting topics to explore further.

To optimize the available flexibility of households using DSM, various device types can be taken into account. Examples of such devices are: dishwashers (DW), washing machines (WM), dryers (DY), heat pumps (HP), electric vehicles (EV), and battery energy storage systems (BESS). In literature, DSM methods are usually explored to control one, or a combination of, these devices. However, DSM methods bring their own challenges both from a technical

and a legislative perspective. These challenges include, but are not limited to:

- **(Dis)comfort** - DSM may, e.g., change the setpoint of a thermostat, which can affect user comfort.
- **Device wearing** - DSM may, e.g., cause additional cycling on EV batteries, affecting their lifetime.
- **Privacy** - DSM may require monitoring of energy consumption of users, potentially revealing sensitive information.
- **Costs** - DSM requires specific hardware, such as smart meters, which may require additional infrastructure costs.

To best procure flexibility in DSM, these barriers must be overcome. Therefore, it is interesting to research which device types are *most interesting* in terms of the added value of their flexibility. To express this value of device flexibility in DSM, a measure that depicts the amount of offered flexibility would be of value.

Gerards and Hurink [12] proposed a method to evaluate the value of flexibility that is offered by different device types within a household, for both peak shaving and the maximization of self consumption. They assess the flexibility of a device compared to its "default mode of operation" where its flexibility is not used. We aim to extend this method by not only evaluating the flexibility of one isolated device, but by evaluating the *average* marginal contribution of devices with all possible subsets of devices. Such a value quantification of *average marginal contributions* of device types is missing in literature to the best of our knowledge.

To systematically compare combinations of device types, we propose to use *Shapley values*. They are a concept originating from the field of game theory, and are used to allocate the total value generated within a cooperative game to its players in a fair manner [28].

Shapley values have been used in recent literature on energy systems to distribute costs/profits among suppliers or prosumers [5, 9, 15, 26] and for redispatch congestion cost allocation [1]. Furthermore, examples of their use can be found with various different fields of research. The Shapley value has been used in policy literature to attribute risk and to derive measures of systemic importance of banks [30], to quantify how effective political parties are at passing bills [6], and even to analyze the WTC 9/11 terrorist attack [34]. Additionally, it has been used in the field of economics for fair profit sharing in e-commerce [22], for supply chain management [35], and to assign prices to climate change risks [8]. In the field of law, it has been proposed as a tool to assign liability [20], to decide who should bear an employee's special annual payment [16], and to determine the best legal method to share the costs of an apartment building elevator [10].

In the field of machine learning (ML) and artificial intelligence (AI), the Shapley value is, among others, used for feature selection, explainability, multi-agent reinforcement learning, ensemble pruning, and data valuation [27]. Through the use of ML/AI, the Shapley value has also gained attention in the field of medicine, e.g., for research in Alzheimer's disease [2, 3]. The widely used SHAP framework, which presents a unified method for interpretation of ML/AI predictions, is also based on Shapley values [23, 31].

The examples above show the versatility of the Shapley value. In this work, we aim to use it in the field of energy management to quantify the value of flexible assets. In the context of a smart

home, Gerards et al. [12] already showed that the flexibility of DW, WM and DY devices provide relatively little benefit on their own compared to BESS and EVs. We will confirm their results through our Shapley value analysis, and additionally, research the potential of *synergy* between assets: this means that we determine which combinations of assets benefit the most from working together. We evaluate the worth of assets and their combinations in a scenario where flexibility is used to minimize the peak grid load of a household, through minimization of the 2-norm of its electricity profile. However, we already note at this point that the presented methodology can easily be adapted for other optimization goals, scenarios and application areas. The main contributions of this paper are:

- A novel methodology for the evaluation of the value of the flexibility offered by different smart device types.
- A framework for evaluation of the synergy of smart device combinations.
- An evaluation of the flexibility of household smart devices for grid peak load minimization in DSM.
- Recommendations of future research directions with regard to device types and device type combinations in DSM for the residential sector.

The remainder of this paper is organized as follows: Section 2 introduces the approach we use to evaluate flexibility. Section 3 describes the scenario used for evaluation, and Section 4 describes how Section 2 and Section 3 can be linked to evaluate flexibility in the context of DSM specifically. Section 5 shows the results of the flexibility value evaluation for individual devices, and Section 6 presents the value of synergy between devices that comes on top of their individual valuations. Finally, in Section 7, we draw conclusions based on the presented results.

## 2 APPROACH

In this section we present a generic methodology to fairly calculate the flexibility value of (sets of) assets. Later, in Section 4, we elaborate on the application of this methodology to the use case of this paper, but the general approach presented in the current section can be applied to other scenarios as well.

We first present a method to quantify the value of the flexibility of a single asset from literature, which is based on marginal contributions. After this, we provide a method to value the interaction or *synergy* between two assets, i.e., the added value of two assets collaborating beyond just the sum of their individual worths. Finally, we present a fairer method to value flexibility of a single asset follows that is based on the Shapley value, which takes into account interaction effects between assets.

### 2.1 Marginal contribution

To quantify the added value of flexibility from (a combination of) assets, we calculate their *marginal contribution* in an approach similar to Gerards and Hurink [12]. The marginal contribution does not take into account interaction effects between different assets, but as the approaches presented later use the marginal contribution, we introduce it here as a starting point.

To begin, let us consider a situation with a set  $N$  of devices (assets) in a household DSM system. To quantify the value of a device  $i \in N$  within the house to the system performance, we

evaluate its marginal contribution  $\xi(i)$  to a subset, or *coalition*,  $S \subseteq N$  of devices. As an example, to find the marginal contribution of a device  $i$  in a house with  $N$  devices, we might consider the coalition  $S = N \setminus \{i\}$ . The marginal contribution  $\xi(i)$  is then defined as:

$$\xi(i) = v(S \cup \{i\}) - v(S), \quad (1)$$

where  $v(S)$  is a function to determine the worth of a coalition  $S \subseteq N \setminus \{i\}$  of devices that are collaborating. In Section 3, we specify this worth for our DSM use-case, but note that the same approach to determine  $\xi(i)$  can be generalized from this example of devices in a household, to any type of assets in a larger system.

While the marginal contribution  $\xi(i)$  can be used to evaluate the added value of an asset  $i$  to a specific coalition  $S$ , it does not specify the average contribution of  $i$  across all possible coalitions  $S$ . This means that an asset might be attributed a value that is unfairly low or high, depending on which specific other assets it was combined with for the evaluation. To illustrate this with the household DSM example, a BESS may have a reduced marginal contribution if there is also an EV available that already provides enough flexibility, while in a DSM system without an EV, the marginal contribution of the BESS would be much larger. Hence, to fairly attribute value to assets, it is necessary to find a measure of how much value is derived from being in a coalition with various other assets.

## 2.2 Synergy

When assets are in a coalition together, the interaction between them may result in a valuation that is higher or lower than merely the sum of the valuation of the two assets individually. Thus, to investigate the added value of interaction between assets, we evaluate their *synergy*. To this end, we use the concept of the interaction index to quantify the worth of interaction effects. In this section, we first introduce an intuitive understanding of synergy between two assets  $i$  and  $j$ , after which we provide a formal definition of the interaction index to quantify synergy.

**2.2.1 Synergy intuition.** Consider assets  $i$  and  $j$ . Intuitively, the interaction index  $\hat{I}_{\{i,j\}}$  between them depends on the difference between the worth of the assets combined  $v(\{i,j\})$ , and the sum of the worth of the separate assets  $v(i) + v(j)$  [11]:

$$\hat{I}_{\{i,j\}} = v(\{i,j\}) - [v(i) + v(j)]. \quad (2)$$

When  $\hat{I}_{\{i,j\}}$  is positive, there is a complementary effect between  $i$  and  $j$ , whereas a negative  $\hat{I}_{\{i,j\}}$  implies negative or redundant interaction. However, for a fair comparison of the contributions of  $i$  and  $j$ , Fujimoto et al. [11] note that not only  $v(\{i,j\})$  and  $[v(i) + v(j)]$  should be compared, but also the effects of  $\{i\}$ ,  $\{j\}$  and  $\{i,j\}$  joining all possible coalitions  $T \subseteq N \setminus \{i,j\}$ . By averaging over all possible coalitions  $T$ , a fair value of the contribution of the synergy between two assets can be achieved.

**2.2.2 Interaction index.** To take into account the combined effect of  $i$  and  $j$  joining different coalitions  $T$ , Owen [25] defined a formal interaction index  $I(v, \{i,j\})$  between  $i$  and  $j$ . This interaction index uses the inclusion-exclusion principle to determine the marginal interaction  $\Delta_{\{i,j\}}v(T)$  between  $i$  and  $j$  in the presence of a coalition  $T$  of assets [14]:

$$\Delta_{\{i,j\}}v(T) := v(T \cup \{i,j\}) - v(T \cup \{i\}) - v(T \cup \{j\}) + v(T). \quad (3)$$

The structure in this equation is similar to (2). In an approach similar to the Shapley value introduced later, we may compute the interaction index  $I(v, \{i,j\})$  using  $\Delta_{\{i,j\}}v(T)$  by:

$$I(v, \{i,j\}) := \sum_{T \subseteq N \setminus \{i,j\}} \frac{1}{n-1} \binom{n-2}{|T|}^{-1} \Delta_{\{i,j\}}v(T). \quad (4)$$

The interaction index between players  $i$  and  $j$  can be understood as the average of the marginal contributions of  $i$  in the presence of  $j$  minus the average of the marginal contributions of  $i$  in the absence of  $j$ , which corresponds to the weighted sum over all coalitions  $T \subseteq N \setminus \{i,j\}$  [24]. We will use  $I(v, \{i,j\})$  as a measure to determine the value of the synergy between two assets  $i$  and  $j$  in the context of a DSM system.

## 2.3 Shapley value

From the above definition of synergy, it follows that there is value in interaction between assets, and additionally, this value changes depending on the presence of other assets. These effects are not taken into account when determining the marginal contribution  $\xi(i)$  of an asset. Thus, to value the contribution of an asset while taking into account its interaction with any set  $S$  of other assets, we derive a method to attribute the *average* marginal contribution of a single asset  $i$  using the Shapley value.

This attribution of worth using average marginal contributions gives a fairer representation of the worth of an asset than the marginal contribution  $\xi(i)$  of Section 2.1 that was also used in [12]. The Shapley value  $\phi_i(v)$  is calculated using the average marginal contribution of  $i$  across all possible subsets  $S \subseteq N$  of assets:

$$\phi_i(v) = \sum_{S \subseteq N \setminus \{i\}} \frac{|S|! (n - |S| - 1)!}{n!} [v(S \cup \{i\}) - v(S)] \quad (5)$$

$$= \sum_{S \subseteq N \setminus \{i\}} \frac{1}{n} \binom{n-1}{|S|}^{-1} [v(S \cup \{i\}) - v(S)], \quad (6)$$

Where each coalition  $S$  is one of the possible combinations of assets in  $N$  and  $|S|$  is the number of assets in  $S$ . Note that the structure of this equation is similar to equation (4).

To calculate the Shapley value, we must consider all possible subsets  $S \subseteq N$  of assets. If we have  $n$  assets in  $N$ , we thus consider  $\mathfrak{S}$  combinations:

$$\mathfrak{S} = 2^n - 1. \quad (7)$$

It becomes clear that the computational complexity of calculating the Shapley value scales exponentially with the number of assets  $n$ .

## 3 TEST METHOD

In this section, we describe the scenario used to evaluate the value of flexible assets in a DSM system. We also describe how the worth  $v(S)$  of a coalition is defined in the remainder of this paper, which is important for the results in the following sections.

### 3.1 Scenario

We first introduce the evaluation scenario, which is used to evaluate the Shapley value of assets, and the synergy between them, in the context of DSM. For our evaluation, we consider the situation of a smart home, but the same methodology could also be applied to other types of systems and/or assets.

**3.1.1 Setup.** We consider a single household, which has the following devices that can be steered through DSM: EV, HP, BESS, DW, and WM. We use the open source DEMKit simulation software [17, 32] for our simulations, combined with the open source load profile generator software ALPG [18, 33], to generate household energy demand patterns and model device flexibility. We simulate a week with weather data from January 2021 in the Netherlands (i.e., cold weather) such that the HP has substantial work to do to keep the house warm.

For a fair attribution of worth to the value of flexibility of a device, we consider scenarios where a device is either behaving greedily when it is not in the coalition (i.e., it follows its default profile), or its flexibility is procured by the DSM algorithm when it is in the coalition. An exception is made for the BESS: As it only makes sense for a BESS to behave in a smart way, it is set to be completely inactive when it is not in the coalition. Section 4 gives a practical example of what it means for devices to be part of a coalition.

**3.1.2 Scope.** In our scenario, we assume we have perfect predictions of weather and household baseload data. The reason for this is that we are interested in the effect of being able to plan the schedule of devices, but not in the robustness of our planning algorithm to prediction inaccuracies. Additionally, we assume that when a device is not controlled, it does not communicate with the DSM algorithm. This implies that, if a device is not controlled, the algorithm is entirely unaware both of when it will consume energy, and how much energy it will consume. While in practical scenarios, uncontrolled devices could (to an extent) be predicted based on historical data, the accuracy of such predictions is outside the scope of this work, and hence we leave it out.

**3.1.3 Computational complexity.** Due to the complexity described in equation (7), it becomes clear that we can only evaluate for a small set of assets, since the exponential scaling of the number of simulations  $\mathfrak{S}$  would quickly become too large to be feasible for evaluation. Hence, we only evaluate for five devices, which, as follows from equation (7), gives 31 combinations of controlled devices to consider, and therefore 31 simulations to run. Each simulation for a week in DEMKit takes roughly 10 seconds to complete on an Intel Core i7-12700H processor, so 31 simulations take 5 minutes.

While this is a reasonable simulation time, the exponential scaling means that it becomes infeasible to increase the number of considered devices beyond a certain number, and is something to take into account for other evaluations. However, we note that such evaluations with many more assets could still be feasible, e.g., when aggregating the flexibility of these assets with methods such as the one presented in [19], or by applying Shapley approximating algorithms such as the random sampling method presented in [7].

### 3.2 Optimization goal & coalition worth

In the following, we elaborate on the worth of a coalition within our simulation framework. To determine this worth, it is important to understand what goal we are optimizing for. For this, we discuss the DSM method that we use for evaluation.

**3.2.1 Optimization goal.** Given a scenario of a single smart house, we aim to minimize the Euclidean norm (2-norm) of the house profile using DSM, i.e., we aim to make the house profile as flat (close to zero) as possible by steering the profiles of the individual devices in a coalition  $S$ .

Since we aim to minimize the Euclidean norm of the house profile, we use the Profile Steering (PS) algorithm for DSM [13]. This algorithm by default optimizes to minimize the Euclidean norm of the profile, which is defined as:

$$\|\vec{x}\|_2 := \sqrt{\sum_{l=1}^L x_l^2}. \quad (8)$$

In this equation,  $\vec{x}$  is the house profile, i.e., the sum of the consumption of the set  $N$  devices in the house, and we evaluate over a time horizon of length  $L$ . Note that if a device is not in the coalition  $S$ , its consumption profile still impacts the house profile; its absence in the coalition only means that its flexibility is not procured to improve the house profile. PS aims to use flexibility to minimize the Euclidean norm  $\|\vec{x}\|_2$  through an iterative planning process. We refer the reader to [13] for more details.

**3.2.2 Coalition worth.** A simple measure for the worth of a coalition of devices  $S$  is how much the Euclidean norm improves compared to when the EMS is not actively procuring the flexibility of the devices in  $S$ , i.e.,

$$v(S) = \|\vec{x}_0\|_2 - \|\vec{x}\|_2. \quad (9)$$

Here,  $\vec{x}_0$  is the worth of the coalition that includes no devices. In other words, it is the case where no flexibility is used to improve the household load profile.

Note that this definition of  $v(S)$  can be applied to compare simulations of the same time horizon and interval step size. However, this definition is not useful to compare results from simulations with a different time horizon and interval size. Thus, to quantify the worth of the coalition, we also have to account for the number of intervals in the simulations. We do this by using the root mean square (RMS) of the profile, similar to [12], which is defined by:

$$M_2(\vec{x}) := \sqrt{\frac{1}{L} \sum_{l=1}^L x_l^2}. \quad (10)$$

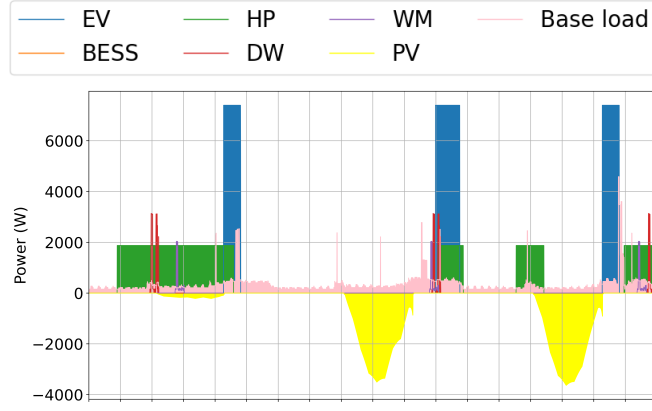
We now define the worth  $v(S)$  of coalition  $S$  as the improvement of  $M_2(\vec{x})$ , compared to when no flexibility is procured from any of the devices in the house:

$$v(S) = M_2(\vec{x}_0) - M_2(\vec{x}). \quad (11)$$

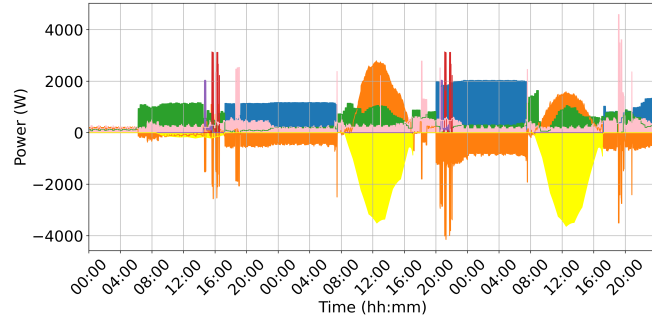
## 4 COALITIONS IN PRACTICE

In the following sections, we show how the approach presented in Section 2 can be applied to the field of energy. However, to be able





(a) Device profiles when none of the devices are part of a coalition, i.e., are not controlled. Note that this scenario excludes the BESS, as explained in Section 3.1.



(b) Device profiles when all devices *are* part of a coalition, i.e., are controlled.

**Figure 2: Two plots of device behavior when they are *not* part of a coalition (2a), and when they *are* in a coalition (2b). We also plot the base load of the house (pink) and photovoltaics (PV, yellow) since these are required to understand the behavior in 2b.**

to position the presented results, it is important to first understand the practical implication of a device being part of a coalition. Thus, we give an **intuition of what it means for devices to be part of a coalition in this section.**

Figure 2a and Figure 2b give an example of how the profiles of devices change when they respectively are, or are not, part of an evaluated coalition  $S$ . In both of the figures, the house profile  $\vec{x}$  is the sum of the profiles plotted. In Figure 2a, none of the devices in our evaluated house are part of  $S$ , meaning they are all uncontrolled. In this situation, they exhibit their default energy usage behavior, resulting in a profile that has considerable peaks. For example, there is hardly any consumption during solar production (in the plots, negative power is production), and the EV charging creates high peaks that are not compensated by PV production or a BESS.

Figure 2b shows the situation where all devices *are* part of  $S$ , i.e., all of them *are* controlled. When a device is part of  $S$ , its power profile is optimized by its controller to make the combined profile of the entire house  $\vec{x}$  as flat (close to zero) as possible. The controllers

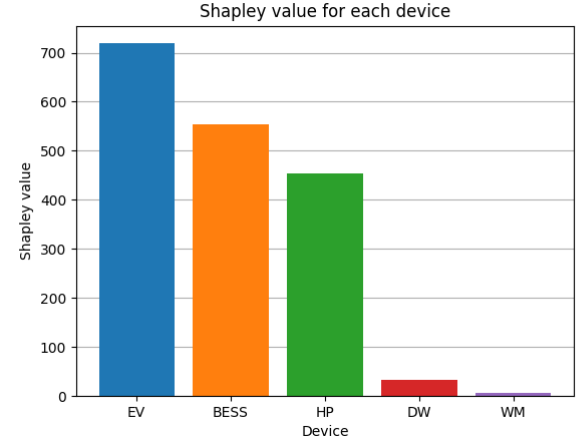


**Figure 3: Shapley values in simulations with an EV of 50kWh (11kW), BESS of 13.5kWh (5kW), and HP with 2.5 kW electrical power.**

steer consumption towards times when there is production, and otherwise try to spread consumption peaks as much as possible. For example, we see that the BESS and HP are steered to consume during the PV production peak, and the EV charging is scheduled to spread the load throughout the night instead of creating a large load peak in the evening. The difference between Figure 2a and Figure 2b shows that when the devices are part of a coalition  $S$ , the resulting house profile  $\vec{x}$  (the sum of the device profiles) may be significantly flatter than in the case where none of the devices are part of  $S$ .

This illustrates the impact of a device being or not being part of a coalition  $S$ .

## 5 SHAPLEY VALUE FOR INDIVIDUAL DEVICES

In this section, we do a valuation of the value of flexibility of devices. We analyze this using the individual Shapley values  $\phi_i$  of the devices, which we determine with the method of Section 2.1 using equation (6). In the evaluation, we consider a house with an EV that has a 50kWh battery and a maximum charging power of 11kW, a BESS of 13.5kWh capacity and 5kW (dis)charge rate, a HP with a maximum electrical power of 3 kW, and a DW and WM whose flexibility can be controlled. We run the simulations with all possible coalitions of these devices to find the Shapley values  $\phi_i$  given in Figure 3. Note that all evaluations are done based on weather data from a winter week, as was previously described in Section 3.1. The results in a summer week may be different, especially for  $\phi_{HP}$ .

We see that  $\phi_{WM}$  and  $\phi_{DW}$  have a relatively low value, meaning the flexibility of the WM and DW only has a relatively low contribution to our goal of Euclidean norm minimization. This is in line with the results found in [12]. In addition to the work of [12], we show in Figure 3 that the value of a HP can roughly be compared to a BESS with the device configurations chosen here.

Note that the results presented in Figure 3 depend on the chosen device configurations. These default device configurations are not

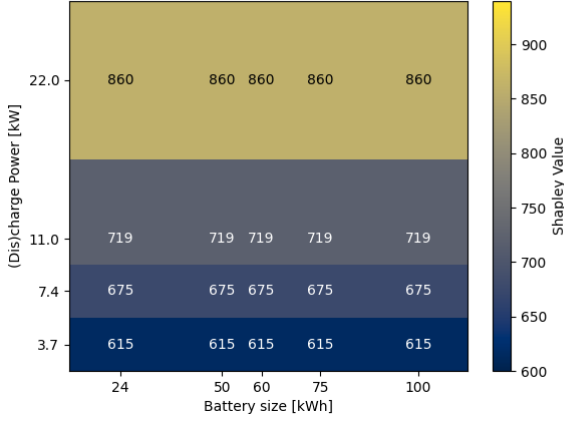


Figure 4: Shapley values for various EV sizes and powers.

representative for every household, while the Shapley value of a device may be highly dependent on its power and/or storage size. For this reason, we compare different configurations for each device in the following subsections, as a means to evaluate the dependence of the Shapley value of a device on its configuration.

### 5.1 EV Shapley value

For EVs, we consider two configuration parameters that can be of influence to their Shapley value  $\phi_{EV}$ : its battery size  $E_{EV}$ , and its maximum charging power  $P_{EV}^{(max)}$ . We consider battery sizes  $E_{EV}$  from 24 kWh to 100 kWh, a range representative of the lower to upper end of the current EV market. For  $P_{EV}^{(max)}$ , we consider 3.7 kW and 7.4 kW as these are the maximum charging powers usually seen for single phase home chargers. Additionally, we present the effect of changing  $P_{EV}^{(max)}$  to 11 kW or 22 kW, as these are common maximum charging powers for EVs that can use three phase chargers. Figure 4 shows the effect of varying  $E_{EV}$  and  $P_{EV}^{(max)}$ .

When looking at  $P_{EV}^{(max)}$ , we see that increasing the maximum EV charging power results in a higher  $\phi_{EV}$ . This follows from the way the worth of a coalition is evaluated. The worth of a coalition is determined based on equation (11). It follows from this equation that the worth of a coalition  $S$  with the EV is evaluated by comparing it to a coalition *without* it. However, note that if the EV is not part of  $S$  (i.e., is not controlled), but has a high  $P_{EV}^{(max)}$ , it will create a very large charging peak. On the other hand, when the EV with high  $P_{EV}^{(max)}$  is part of  $S$ , and its charging demand is spread over the night, the peak can be flattened significantly.

The optimal profile to flatten the peak of  $\vec{x}$  is the same for any EV considered, regardless of its  $P_{EV}^{(max)}$ . As long as this optimal profile of the controlled EV  $\vec{x}_{EV}$  does not exceed  $P_{EV}^{(max)}$  on any interval, the exact value  $P_{EV}^{(max)}$  of a specific EV that is evaluated is of no consequence for  $\vec{x}_{EV}$ . As a result,  $M_2(\vec{x})$ , i.e., the controlled profile, also remains the same in this situation. However, the uncontrolled profile  $M_2(\vec{x}_0)$  is different, since a higher  $P_{EV}^{(max)}$  results in a higher

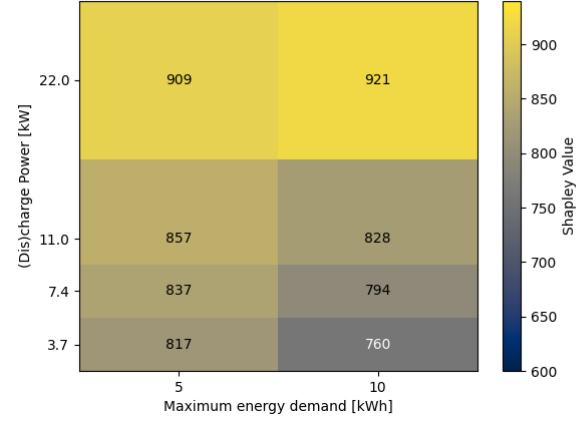


Figure 5: Shapley values for EVs with reduced maximum demand per charging session.

peak and consequentially, a higher value of  $M_2(\vec{x}_0)$ . This implies that the worth  $v(S)$  of a coalition with an EV increases as  $P_{EV}^{(max)}$  increases.

When looking at the effect of varying  $E_{EV}$ , we see that it has no effect on  $\phi_{EV}$  in the evaluated scenario. This is because in general, the energy demand in each day is less than 24 kWh (the smallest evaluated battery size). Thus, a larger battery does not change the demanded energy of the EV in the week that is simulated.

To explain how a change in *demanded energy* instead of battery size influences  $\phi_{EV}$ , we set a limit to the maximum energy an EV may demand in a charging session. This is plotted in Figure 5. In the figure, we see that in general, when an EV has a reduced demand, its Shapley value increases. A smaller demand means the EV needs to charge less and can therefore be more flexible with the time where it charges. From a mathematical view, this effect is again caused by the definition of worth: with less demand, both the uncontrolled EV charging peak, and the controlled charging profile, decrease in total volume. Since we evaluate based on the quadratic two-norm of equation (8), the uncontrolled charging peak is punished harsher than the controlled load spread over the night, implying that if both are smaller, the worth increases.

### 5.2 BESS Shapley value

Figure 6 shows the effect of varying the BESS storage size  $E_{BESS}$  and (dis)charge power  $P_{BESS}^{(max)}$ . We see an overall trend where an increase in either BESS size and/or (dis)charge power results in a higher  $\phi_{BESS}$ . In the case of increasing  $E_{BESS}$ , this trend is always there, but for  $P_{BESS}^{(max)}$ , the highest (dis)charge power does *not* get the highest  $\phi_{BESS}$ .

This can be explained by the behavior of the BESS when it is acting in a coalition that does not contain the EV (i.e., the EV is not controlled). When the EV is not controlled, it does not communicate with the DSM algorithm, which means the algorithm is unaware of the arrival/departure time or required energy of the EV, as explained

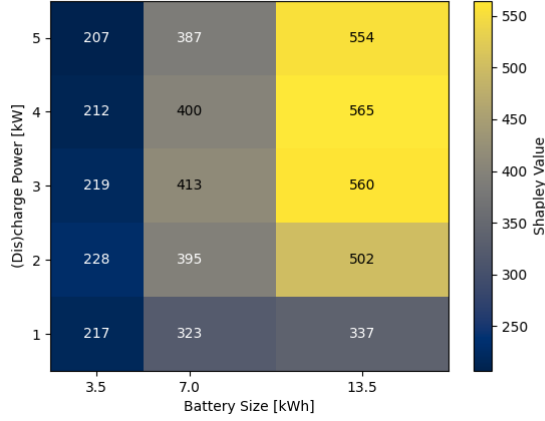


Figure 6: Shapley values for various BESS sizes and powers.

in Section 3.1.2. Thus, when the EV arrives, the best the algorithm can do is to use the BESS to minimize the peak of the EV charging as much as possible. If the BESS holds more energy than the EV requires, this is a good strategy, but in many cases, the BESS will run out of charge before the EV is fully charged. An example of this is given in Figure 7: The BESS (orange) is used to minimize the peak caused by an (uncontrolled) EV (blue) as much as possible as soon as the EV starts charging, but runs out of charge before the charging session is finished.

This effect becomes more pronounced as  $|P_{BESS}^{(max)}|$  increases, since the BESS fully drains sooner when it can discharge itself faster. If the BESS would have been planned such that it had spread its capacity over the entire charging session, the resulting profile would have been flatter, and the Shapley value would have increased, but when the EV is not part of the coalition (i.e., it is charging greedily), this is not realistic. Because this negative effect of increasing  $|P_{BESS}^{(max)}|$  weighs stronger than the positive effect of a high  $|P_{BESS}^{(max)}|$  when the BESS is in a coalition together with a smart charging EV,  $\phi_{BESS}$  decreases slightly in the presented results when  $|P_{BESS}^{(max)}|$  increases beyond a certain threshold.

### 5.3 HP Shapley value

Figure 8 presents the effect of varying the maximum power  $P_{HP}^{(max)}$  of a HP. It shows that the Shapley value of the HP  $\phi_{HP}$  is only affected by  $P_{HP}^{(max)}$  when  $P_{HP}^{(max)}$  is small, and even then the change in  $\phi_{HP}$  is small. The reason for this is that the maximum capacity of a HP is rarely used in our scenario, even when the HP is uncontrolled. Thus, the value of flexibility of a HP remains mostly the same, regardless of the chosen power. This implies that in general, the valuation of HP flexibility is only affected by changing its maximum power, when the maximum power of the HP is already a limiting factor.

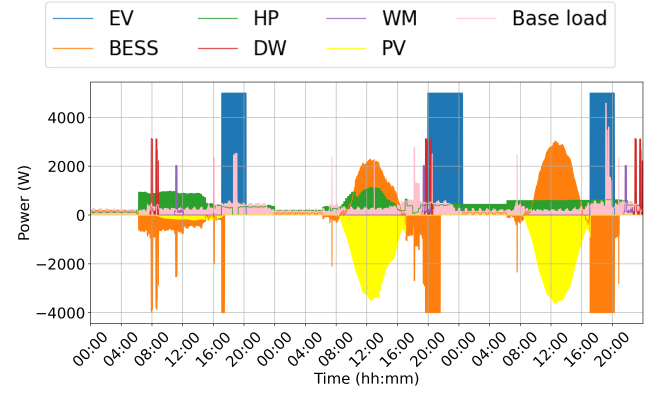


Figure 7: An example of suboptimal BESS planning in the simulation software.

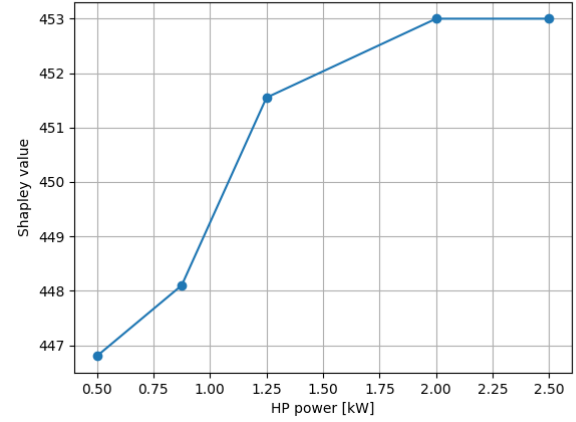


Figure 8: Shapley values for various HP powers.

### 5.4 WM and DW Shapley value

While both the Shapley values  $\phi_{WM}$  and  $\phi_{DW}$  are relatively small compared to the other  $\phi_i$  values in our evaluation, we still see a significant difference between  $\phi_{WM}$  and  $\phi_{DW}$  when we ignore the other devices.  $\phi_{DW}$  is more than 4 times as large as  $\phi_{WM}$ . This can be explained by the energy consumption of the devices themselves: the evaluated DW has an energy consumption that is much higher than the energy consumption of the WM. Thus, controlling the greater load of the DW provides more opportunities to flatten the house load than controlling the smaller load of the WM.

If we were to consider a more energy-efficient DW and a less energy-efficient WM, the differences between  $\phi_{WM}$  and  $\phi_{DW}$  would change accordingly and the WM might have a higher Shapley value than the DW. However, because of the relatively small significance of the WM and DW compared to the other devices, we do not elaborate on the effect of energy efficiency in DWs and WMs further in this work.

## 6 SYNERGY BETWEEN DEVICES

In this section, we consider the worth of the coalitions to determine the synergy between devices as defined in Section 2.2. The synergy between devices within our scenario is visualized in heatmaps in Figure 9. The plots, based on equation (2), show the synergy  $I(v, \{i, j\})$  between devices  $i$  and  $j$ , where device  $i$  is plotted on the x-axis and device  $j$  on the y-axis.

Figure 9 shows two heatmaps because the synergy between devices is highly dependent on the characteristics of the devices themselves, as becomes clear when comparing Figure 9a and Figure 9b. Changing the characteristics of one of the devices affects the synergy between the devices in the house. Because the EV has the highest Shapley value and thus likely has the most impact, we vary the EV configuration first, and see how this affects the synergy between the EV and other devices. Afterwards, we discuss synergy between devices other than the EV.

### 6.1 Synergy between EV and BESS

Figure 9a shows that when we have an EV with a high  $P_{EV}^{(max)}$ , the synergy between EV and BESS is negative. A negative synergy implies that the sum of the flexibility value of the individual devices is greater than the flexibility value of controlling both devices simultaneously. The meaning of a negative synergy can be explained using (3), which shows there are four factors influencing synergy between two devices  $i$  and  $j$ :

- $v(T \cup \{i, j\})$ , the worth of a coalition that includes both  $i$  and  $j$ .
- $v(T \cup \{i\})$ , the worth of a coalition that includes  $i$  but not  $j$ .
- $v(T \cup \{j\})$ , the worth of a coalition that includes  $j$  but not  $i$ .
- $v(T)$ , the worth of a coalition that includes neither  $i$  nor  $j$ .

The cause of this negative synergy between an EV and a BESS when the EV has a high  $P_{EV}^{(max)}$ , can be explained by what happens when the EV is not part of a coalition. In this situation, the EV creates a high peak, the height of which is determined by  $P_{EV}^{(max)}$ . To cope with this peak in a coalition  $T \cup \{BESS\}$  that includes the BESS, the flexibility of the BESS is then used almost exclusively to decrease the severity of the EV charging peak. Decreasing the charging peak instead of other (smaller) peaks provides the best improvement in terms of the optimization goal of (8), and therefore, provides the best improvement in worth. In the same situation but without the BESS, i.e., coalition  $T$ , not much can be done about the EV peak, and the worth of the coalition is low.

When the EV is part of a coalition  $T \cup \{EV\}$ , it provides a high worth by spreading the most imminent peak in the profile: its own peak. This happens regardless of the presence of the BESS in a coalition, since in any coalition, the EV is first decreasing its own peak.

This goes back to the same argument that was also mentioned in Section 5.1. The profile of coalitions  $T \cup \{EV\}$  is the same regardless of  $P_{EV}^{(max)}$ , since the optimal controlled profile of the EV is the same regardless of  $P_{EV}^{(max)}$ . As a result, the profile of  $T \cup \{EV, BESS\}$  is also always the same regardless of  $P_{EV}^{(max)}$  in any of the scenarios evaluated.

We can thus conclude that when determining the synergy between EV and BESS, the first two terms of (3) are always equal to some constant  $C$  for a given coalition  $T$ , regardless of the value of  $P_{EV}^{(max)}$ :

$$v(T \cup \{EV, BESS\}) - v(T \cup \{EV\}) = C \quad \forall P_{EV}^{(max)}. \quad (12)$$

It follows that the synergy between BESS and EV only depends on  $v(T \cup \{BESS\})$  and  $v(T)$ , where the first has a negative effect on synergy and the latter a positive effect. When  $P_{EV}^{(max)}$  increases,  $v(T \cup \{BESS\})$  also increases significantly, an indication that the BESS is mitigating the EV peak. However, as  $v(T \cup \{BESS\})$  contributes negatively, this effect *decreases* the synergy. Meanwhile,  $v(T)$  does not show a significant change, as  $T$  does not contain any devices with flexibility that can decrease the EV peak substantially. This explains why we see a decrease in synergy between BESS and EV when  $P_{EV}^{(max)}$  increases, and vice-versa.

### 6.2 Synergy between EV and HP

Besides the EV, other devices, such as the HP, also show interesting synergy effects. These effects also vary depending on the BESS configuration and on  $P_{EV}^{(max)}$ . Figure 10 shows that when we decrease the BESS power and capacity, different synergy patterns emerge.

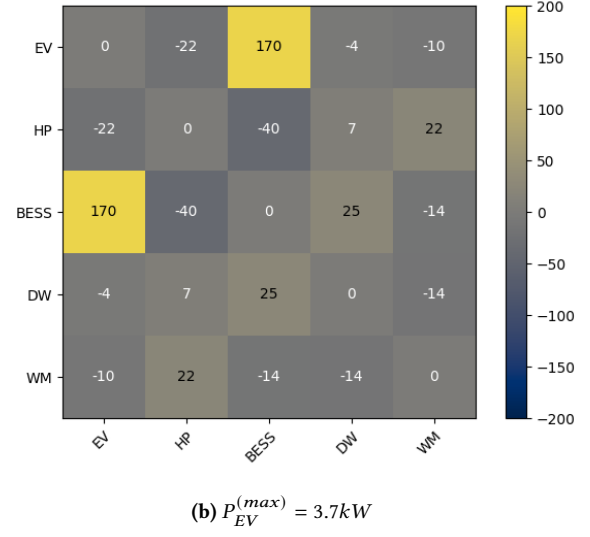
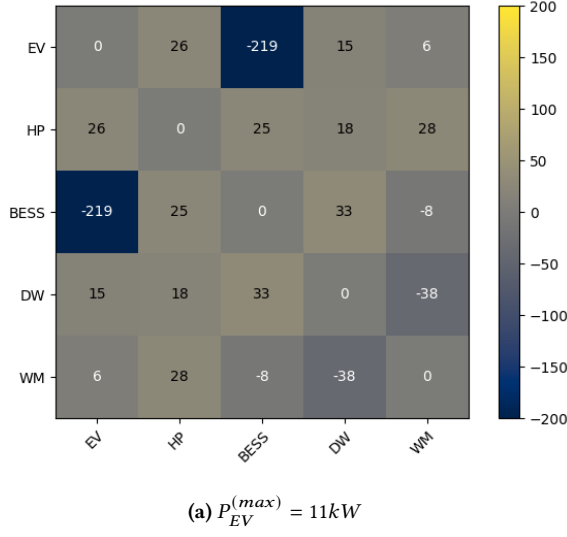
The device that sees the most noticeable increase in synergy with the EV when the BESS power and capacity are reduced, is the HP. This is because the worths  $v(T \cup \{EV\})$  and  $v(T \cup \{HP\})$  are both low, a result of the lack of communication between EV and HP when one or the other is not part of the coalition. If the EV is not in the coalition, the HP is not aware of the EV profile, and the HP profile will not be adapted to the EV peak. The same effect occurs when the EV is in the coalition while the HP is not.

Thus, the negative contributions both have a relatively low worth. On the other hand, when both EV and HP are in a coalition, they can change their profiles to adapt to each other. This is shown in Figure 11, where the HP plans its consumption around the EV charging as much as possible. As a result,  $v(T \cup \{EV, HP\})$  is significantly higher in comparison to  $v(T \cup \{EV\})$  and  $v(T \cup \{HP\})$ , and thus the interaction index  $I(v, \{EV, HP\})$  increases. When we consider the same interaction but with a stronger BESS, this synergy is significantly less, as the BESS will account for many of the overlapping peaks of the non-controlled EV and/or HP. Thus, smartly controlling a HP and an EV together can provide synergy benefits that come on top of the benefits of controlling them individually, but the effect is most pronounced in situations where there is no strong BESS.

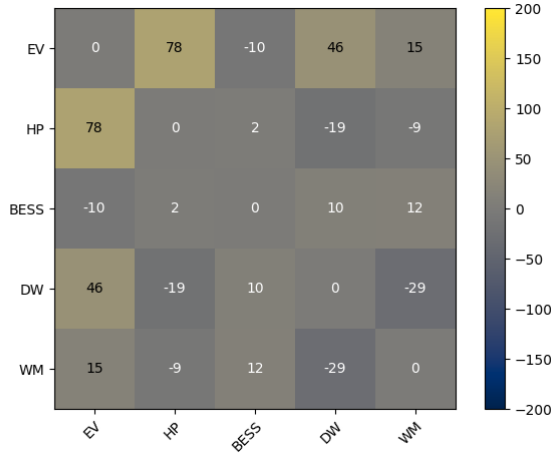
### 6.3 Synergies with DW and WM

Figure 9 and Figure 10 show that the DW and WM have a negative synergy with each other in all evaluated scenarios. The cause of this is that both can provide similar benefits when they are part of a coalition. Consequently, following the law of diminishing returns, having both of them in the same coalition is not worth as much as having one of them separate. What is interesting however, is that similar to the HP, the synergy between DW/WM and EV increases when there is no strong BESS, as becomes clear when comparing





**Figure 9: Interaction index  $I(v, \{i, j\})$  between devices as measure of synergy.** The two plots represent two different values of  $P_{EV}^{(max)}$ , all other devices are on their default values, i.e., the values mentioned in the beginning of Section 5. Notice that the heatmaps are symmetrical on the diagonal.



**Figure 10: Synergy with a less powerful BESS but high EV power:**  $P_{EV}^{(max)} = 11kW$ ,  $E_{BESS} = 3.5kWh$ ,  $|P_{BESS}^{(max)}| = 1kW$ .

Figure 9a and Figure 10. Especially the DW shows a strong synergy with the EV in Figure 10.

## 7 CONCLUSION

This paper introduced a novel framework for evaluation of the flexibility offered by assets and combinations of assets in a DSM context. The presented methodology uses the average marginal contribution of an asset to assign a fair value to its flexibility, taking into account all possible coalitions in which the flexibility could be provided. As a result, the presented method provides a fairer method to evaluate the flexibility of DSM assets than other methods

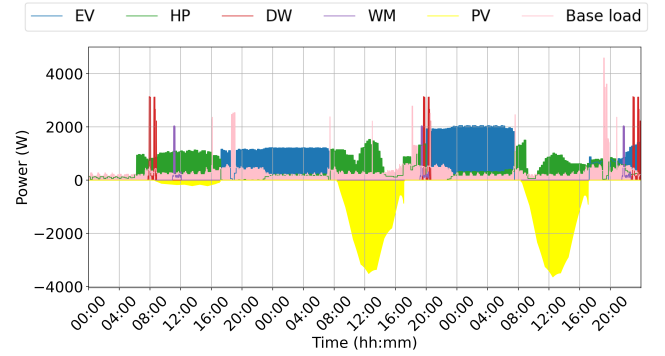


**Figure 11: An example of the HP (green) planning most of its consumption around charging sessions of the EV (blue).** Other devices besides the EV and HP are not controlled here.

already found in literature, which only evaluate assets in a specific coalition.

We have shown in the paper that in the context of flattening the electricity consumption profile of a household in winter, an EV is the most important asset to control, even more important than a BESS. While the BESS is available all day and thus intuition might say it provides higher flexibility, the largest consumption peak of a household is caused by the charging of an EV. This peak is substantially higher than any other peaks caused by other devices, and since the EV *must* charge, its flexibility is more important than the flexibility of a BESS, which does not have such strict requirements. This is why control of an EV is more important than the availability of a BESS in household DSM.

Additionally, we show that there can be strong synergy between devices in a household DSM context. Especially between an EV and a BESS, strong synergy may be found, where the BESS can store solar energy by day to supply to the EV charging session later. However, the synergy between these two devices strongly depends on their maximum (dis)charge powers. When an EV has a high charging power, this negatively affects its synergy with a battery, due to the profile that results from the EV *not* being controlled. This does not necessarily mean that the profile of controlling both an EV with high maximum charging power in combination with a BESS is worse than controlling a BESS and an EV with a lower maximum charging power. Their individual contributions increase as the EV maximum charging power increases, and therefore the resulting profile is still flatter. Nonetheless, the synergy, i.e., the added value of combining BESS an EV besides just their *individual contributions*, may decrease and even become negative. This is further explained in Section 6.1.

While control of an EV, required to mitigate an EV peak, is the most important asset available in household winter load flattening, BESS and HP systems can also provide a significant value with their flexibility, while a DW or WM have significantly less impact. Depending on the chosen device configurations, combinations of devices can provide additional impact on top of the individual value of devices. Therefore, we recommend research and policy in the field of DSM in the residential sector to focus mainly on EV, BESS and HP, and on combinations thereof.

In this paper, the presented approach is applied to devices in a smart house, and the results presented here were obtained. However, it is important to note that the same method can also be applied to other levels in the electricity system. As an example, when comparing flexibility aggregators, the presented approach can highlight an aggregator that can offer flexibility at times where the others cannot, even if that aggregator only offers limited flexibility in an absolute sense. For such an evaluation, the computational complexity of calculating the Shapley value must be taken into account, but when limiting the amount of devices or parties that are evaluated, or by aggregating them, the presented approach can be feasible and provides a fair valuation, making the presented work valuable to various use cases.

## ACKNOWLEDGMENTS

This research is part of the research program ‘MegaMind - Measuring, Gathering, Mining and Integrating Data for Self-management in the Edge of the Electricity System’, (partly) financed by the Dutch Research Council (NWO) through the Perspectief program under number P19-25.

## REFERENCES

- [1] Rebecca Bauer, Xinliang Dai, and Veit Hagenmeyer. 2023. A Shapley value-based Distributed AC OPF Approach for Redispatch Congestion Cost Allocation. In *Proceedings of the 14th ACM International Conference on Future Energy Systems (e-Energy '23)*. Association for Computing Machinery, New York, NY, USA, 109–113. <https://doi.org/10.1145/3575813.3576881>
- [2] Louise Bloch, Christoph M. Friedrich, and for the Alzheimer's Disease Neuroimaging Initiative. 2021. Data analysis with Shapley values for automatic subject selection in Alzheimer's disease data sets using interpretable machine learning. *Alzheimer's Research & Therapy* 13, 1 (Sept. 2021), 155. <https://doi.org/10.1186/s13195-021-00879-4>
- [3] B. Braithwaite, J. Paananen, H. Taipale, A. Tanskanen, J. Tiihonen, S. Hartikainen, and A.-M. Tolppanen. 2020. Detection of medications associated with Alzheimer's disease using ensemble methods and cooperative game theory. *International Journal of Medical Informatics* 141 (Sept. 2020), 104142. <https://doi.org/10.1016/j.ijmedinf.2020.104142>
- [4] Christian Bussar, Philipp Stöcker, Zhuang Cai, Luiz Moraes Jr., Dirk Magnor, Pablo Wiernes, Niklas van Bracht, Albert Moser, and Dirk Uwe Sauer. 2016. Large-scale integration of renewable energies and impact on storage demand in a European renewable power system of 2050—Sensitivity study. *Journal of Energy Storage* 6 (May 2016), 1–10. <https://doi.org/10.1016/j.est.2016.02.004>
- [5] Wenqi Cai, Arash Bahari Kordabad, and Sébastien Gros. 2023. Energy management in residential microgrid using model predictive control-based reinforcement learning and Shapley value. *Engineering Applications of Artificial Intelligence* 119 (March 2023), 105793. <https://doi.org/10.1016/j.engappai.2022.105793>
- [6] A. Casajus and F. Huettner. 2019. The Coleman–Shapley index: being decisive within the coalition of the interested. *Public Choice* 181, 3–4 (2019), 275–289. <https://doi.org/10.1007/s11127-019-00654-y>
- [7] Javier Castro, Daniel Gómez, and Juan Tejada. 2009. Polynomial calculation of the Shapley value based on sampling. *Computers & Operations Research* 36, 5 (May 2009), 1726–1730. <https://doi.org/10.1016/j.cor.2008.04.004>
- [8] Roger M. Cooke. 2011. A Shapley Value Approach to Pricing Climate Risks. <https://doi.org/10.2139/ssrn.1972777>
- [9] Sho Cremers, Valentin Robu, Daan Hofman, Titus Naber, Kavin Zheng, and Sonam Norbu. 2022. Efficient methods for approximating the shapley value for asset sharing in energy communities. In *Proceedings of the Thirteenth ACM International Conference on Future Energy Systems (e-Energy '22)*. Association for Computing Machinery, New York, NY, USA, 320–324. <https://doi.org/10.1145/3538637.3538861>
- [10] Bertrand Crettez and Régis Deloche. 2019. A Law-and-Economics Perspective on Cost-Sharing Rules for a Condo Elevator. *Review of Law & Economics* 15, 2 (July 2019), 20160001. <https://doi.org/10.1515/rle-2016-0001> Publisher: De Gruyter.
- [11] Katsushige Fujimoto, Ivan Kojadinovic, and Jean-Luc Marichal. 2006. Axiomatic characterizations of probabilistic and cardinal-probabilistic interaction indices. *Games and Economic Behavior* 55, 1 (April 2006), 72–99. <https://doi.org/10.1016/j.geb.2005.03.002>
- [12] Marco E. T. Gerards and Johann L. Hurink. 2017. On the value of device flexibility in smart grid applications. In *2017 IEEE Manchester PowerTech*. IEEE, Manchester, United Kingdom, 1–6. <https://doi.org/10.1109/PTC.2017.7981170>
- [13] Marco E. T. Gerards, Hermen A. Toersche, Gerwin Hoogsteen, Thijs van der Klauw, Johann L. Hurink, and Gerard J. M. Smit. 2015. Demand side management using profile steering. In *2015 IEEE Eindhoven PowerTech*. 1–6. <https://doi.org/10.1109/PTC.2015.7232328>
- [14] Michel Grabisch, Jean-Luc Marichal, and Marc Roubens. 2000. Equivalent Representations of Set Functions. *Mathematics of Operations Research* 25, 2 (May 2000), 157–178. <https://doi.org/10.1287/moor.25.2.157.12225> Publisher: INFORMS.
- [15] Liyang Han, Thomas Morstyn, and Malcolm McCulloch. 2021. Estimation of the Shapley Value of a Peer-to-peer Energy Sharing Game Using Multi-Step Coalitional Stratified Sampling. *International Journal of Control, Automation and Systems* 19, 5 (May 2021), 1863–1872. <https://doi.org/10.1007/s12555-019-0535-1>
- [16] Tobias Hiller. 2021. Who Bears an Employee's Special Annual Payment? *Review of Law & Economics* 17, 1 (March 2021), 223–237. <https://doi.org/10.1515/rle-2019-0022> Publisher: De Gruyter.
- [17] Gerwin Hoogsteen, Johann L. Hurink, and Gerard J. M. Smit. 2019. DEMKit: a Decentralized Energy Management Simulation and Demonstration Toolkit. In *2019 IEEE PES Innovative Smart Grid Technologies Europe (ISGT-Europe)*. 1–5. <https://doi.org/10.1109/ISGTEurope.2019.8905439>
- [18] Gerwin Hoogsteen, Albert Molderink, Johann L. Hurink, and Gerard J. M. Smit. 2016. Generation of flexible domestic load profiles to evaluate Demand Side Management approaches. In *2016 IEEE International Energy Conference (ENERGYCON)*. 1–6. <https://doi.org/10.1109/ENERGYCON.2016.7513873>
- [19] Gerwin Hoogsteen, Leoni Winschermann, Bart Nijenhuis, Nataly Bañol Arias, and Johann L. Hurink. 2023. Robust and Predictive Charging of Large Electric Vehicle Fleets in Grid Constrained Parking Lots. In *2023 IEEE International Conference on Communications, Control, and Computing Technologies for Smart Grids (SmartGridComm)*. 1–6. <https://doi.org/10.1109/SmartGridComm57358.2023.10333900> ISSN: 2474-2902.
- [20] Jeong-Yoo Kim and Seewoo Lee. 2019. Apportionment of liability by the stochastic Shapley value. *International Review of Law and Economics* 60 (Dec. 2019), 105860. <https://doi.org/10.1016/j.irle.2019.105860>
- [21] J. G. Kirkerud, N. O. Nagel, and T. F. Bolkesjø. 2021. The role of demand response in the future renewable northern European energy system. *Energy* 235 (Nov. 2021), 121336. <https://doi.org/10.1016/j.energy.2021.121336>
- [22] Jia-Cai Liu and Deng-Feng Li. 2022. Improved Shapley Values Based on Players' Least Square Contributions and Their Applications in the Collaborative Profit Sharing of the Rural E-commerce. *Group Decision and Negotiation* 31, 1 (Feb. 2022), 7–22. <https://doi.org/10.1007/s10726-021-09741-2>
- [23] Scott M. Lundberg and Su-In Lee. 2017. A unified approach to interpreting model predictions. In *Proceedings of the 31st International Conference on Neural*

- Information Processing Systems (NIPS'17)*. Curran Associates Inc., Red Hook, NY, USA, 4768–4777.
- [24] Jean-Luc Marichal and Marc Roubens. 1999. The Chaining Interaction Index among Players in Cooperative Games. In *Advances in Decision Analysis*, R. Lowen, Nadine Meskens, and Marc Roubens (Eds.). Vol. 4. Springer Netherlands, Dordrecht, 69–85. [https://doi.org/10.1007/978-94-017-0647-6\\_5](https://doi.org/10.1007/978-94-017-0647-6_5) Series Title: Mathematical Modelling: Theory and Applications.
  - [25] Guillermo Owen. 1972. Multilinear Extensions of Games. *Management Science* 18, 5-part-2 (Jan. 1972), 64–79. <https://doi.org/10.1287/mnsc.18.5.64> Publisher: INFORMS.
  - [26] Victor M.J.J. Reijnders, Marco E.T. Gerards, and Johann L. Hurink. 2019. Pricing Mechanism Based on Losses Using Grid Topology. In *2019 IEEE Milan PowerTech*. 1–6. <https://doi.org/10.1109/PTC.2019.8810436>
  - [27] Benedek Rozemberczki, Lauren Watson, Péter Bayer, Hao-Tsung Yang, Olivér Kiss, Sebastian Nilsson, and Rik Sarkar. 2022. The Shapley Value in Machine Learning. In *Proceedings of the Thirty-First International Joint Conference on Artificial Intelligence, IJCAI-22*, Vol. 6. International Joint Conferences on Artificial Intelligence Organization, 5572–5579. <https://doi.org/10.24963/ijcai.2022/778> ISSN: 1045-0823.
  - [28] L. S. Shapley. 1953. 17. A Value for n-Person Games. In *Contributions to the Theory of Games (AM-28), Volume II*, Harold William Kuhn and Albert William Tucker (Eds.). Princeton University Press, 307–318. <https://doi.org/10.1515/9781400881970-018>
  - [29] Lennart Söder, Peter D. Lund, Hardi Koduvere, Torjus Folsland Bolkesjø, Geir Høyvik Rossebø, Emilie Rosenlund-Soysal, Klaus Skytte, Jonas Katz, and Dagnija Blumberga. 2018. A review of demand side flexibility potential in Northern Europe. *Renewable and Sustainable Energy Reviews* 91 (Aug. 2018), 654–664. <https://doi.org/10.1016/j.rser.2018.03.104>
  - [30] Nikola Tarashev, Kostas Tsatsaronis, and Claudio Borio. 2016. Risk Attribution Using the Shapley Value: Methodology and Policy Applications \*. *Review of Finance* 20, 3 (May 2016), 1189–1213. <https://doi.org/10.1093/rof/rfv028>
  - [31] Che-Ping Tsai, Chih-Kuan Yeh, and Pradeep Ravikumar. 2023. Faith-Shap: The Faithful Shapley Interaction Index. *Journal of Machine Learning Research* 24, 94 (2023), 1–42. <https://doi.org/10.48550/arxiv.2203.00870>
  - [32] University of Twente - Energy Research Group. 2023. Decentralized Energy Management toolKit (DEMKit). <https://github.com/utwente-energy/demkit>
  - [33] University of Twente - Energy Research Group. 2024. Artificial load profile generator (ALPG). <https://github.com/utwente-energy/alpg>
  - [34] Tjeerd van Campen, Herbert Hamers, Bart Husslage, and Roy Lindelauf. 2017. A new approximation method for the Shapley value applied to the WTC 9/11 terrorist attack. *Social Network Analysis and Mining* 8, 1 (Dec. 2017), 12. <https://doi.org/10.1007/s13278-017-0480-z>
  - [35] Xiao-Xue Zheng, Deng-Feng Li, Zhi Liu, Fu Jia, and Jiu-H-Bing Sheu. 2019. Coordinating a closed-loop supply chain with fairness concerns through variable-weighted Shapley values. *Transportation Research Part E: Logistics and Transportation Review* 126 (June 2019), 227–253. <https://doi.org/10.1016/j.tre.2019.04.006>